

---

# **Semiconductor Devices**

**THIRD EDITION**

**S. M. Sze and M. K. Lee**

---

## **Chapter 8**

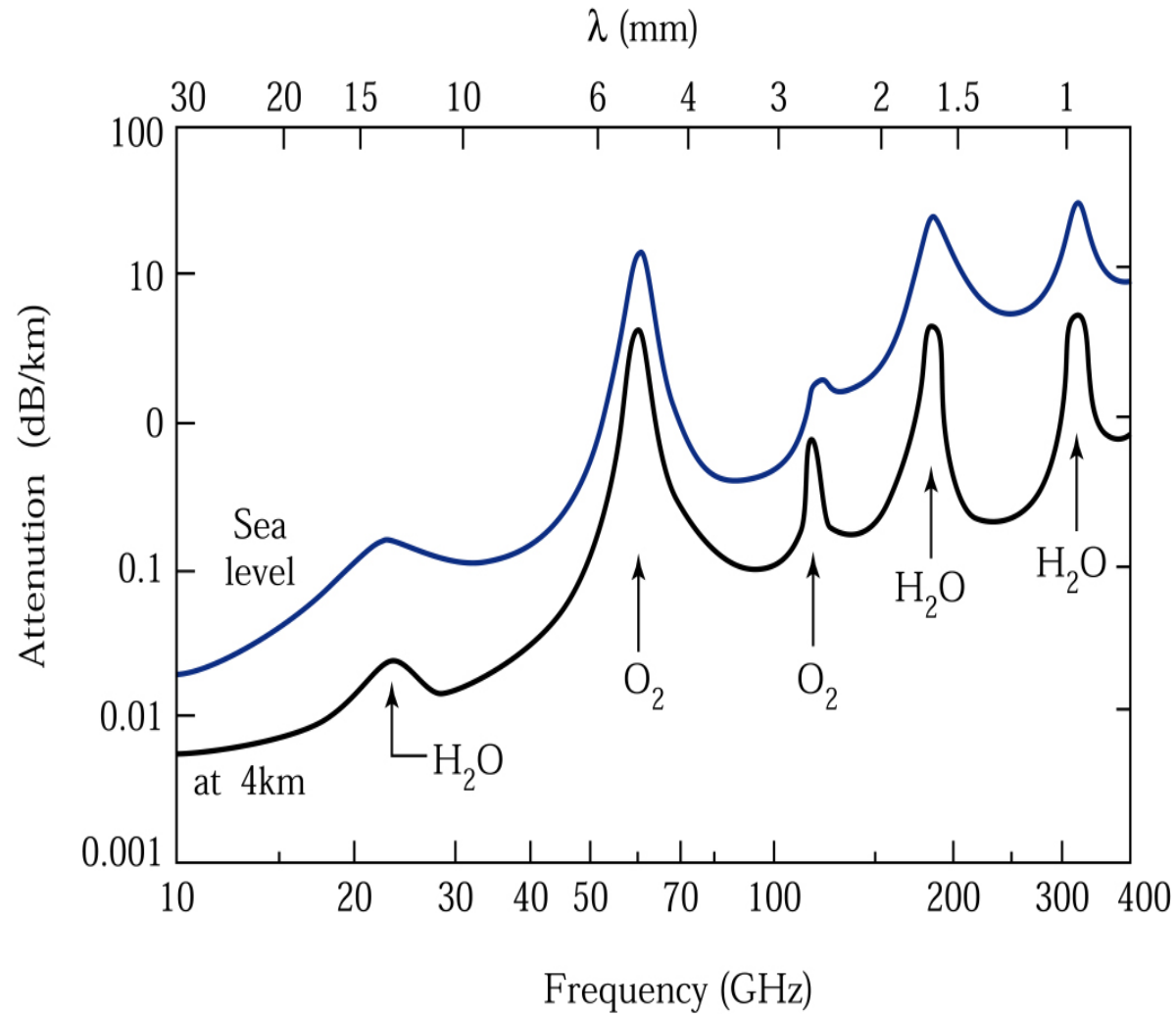
**Microwave Diodes, Quantum-Effect and  
Hot-Electron Devices**

**TABLE 1 IEEE MICROWAVE FREQUENCY BANDS**

Designation	Frequency range (GHz)	Wavelength (cm)
VHF	0.1– 0.3	300.00–100.00
UHF	0.3–1.0	100.00–30.00
L band	1.0–2.0	30.00–15.00
S band	2.0–4.0	15.00–7.50
C band	4.0–8.0	7.50–3.75
X band	8.0–13.0	3.75–2.31
Ku band	13.0–18.0	2.31–1.67
K band	18.0–28.0	1.67–1.07
Ka band	28.0–40.0	1.07–0.75
Millimeter	30.0–300.0	1.00–0.10
Submillimeter	300.0–3000.0	0.10–0.01

**Table 8.1**

© John Wiley &amp; Sons, Inc. All rights reserved.



**Absorption min. are at 35, 94, 140, and 220 GHz**

Average atmosphere absorption of millimeter waves.<sup>4</sup> The upper curve is at the sea level; the lower curve is at 4 km above the sea level.

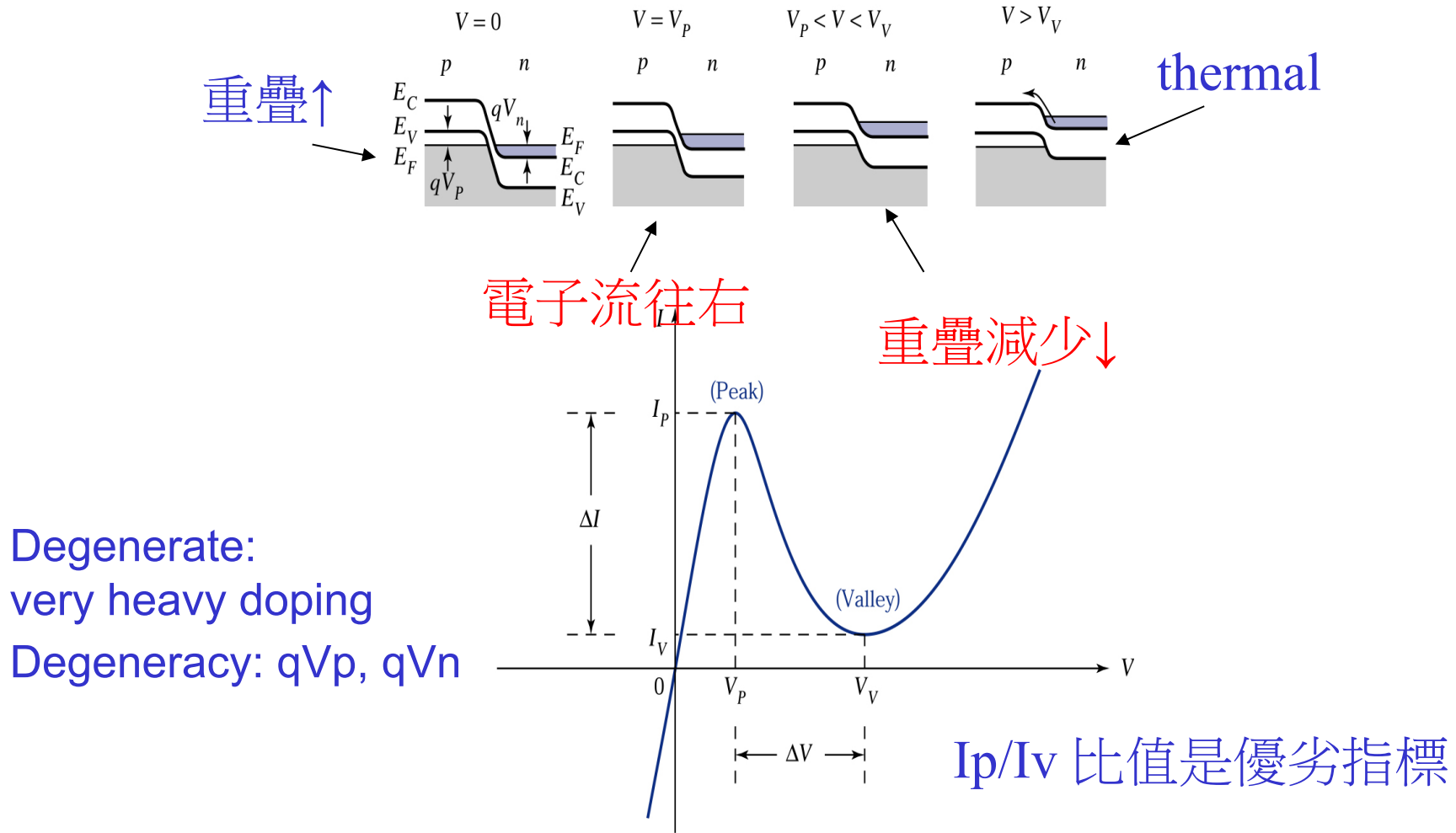


**Figure 8.1.** Static current-voltage characteristics of a typical tunnel diode.  $I_p$  and  $V_p$  are the peak current and peak voltage, respectively.  $I_v$  and  $V_v$  are the valley current and valley voltage, respectively. The upper figures show the band diagrams of the device at different bias voltages.

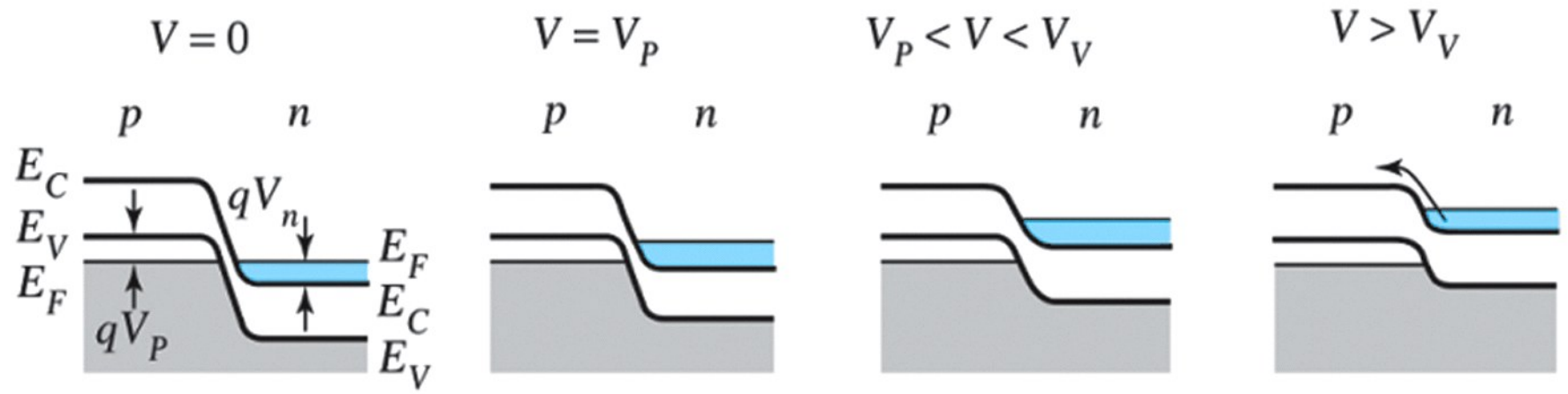


**Figure 8.1 part 1**  
 © John Wiley & Sons, Inc. All rights reserved.

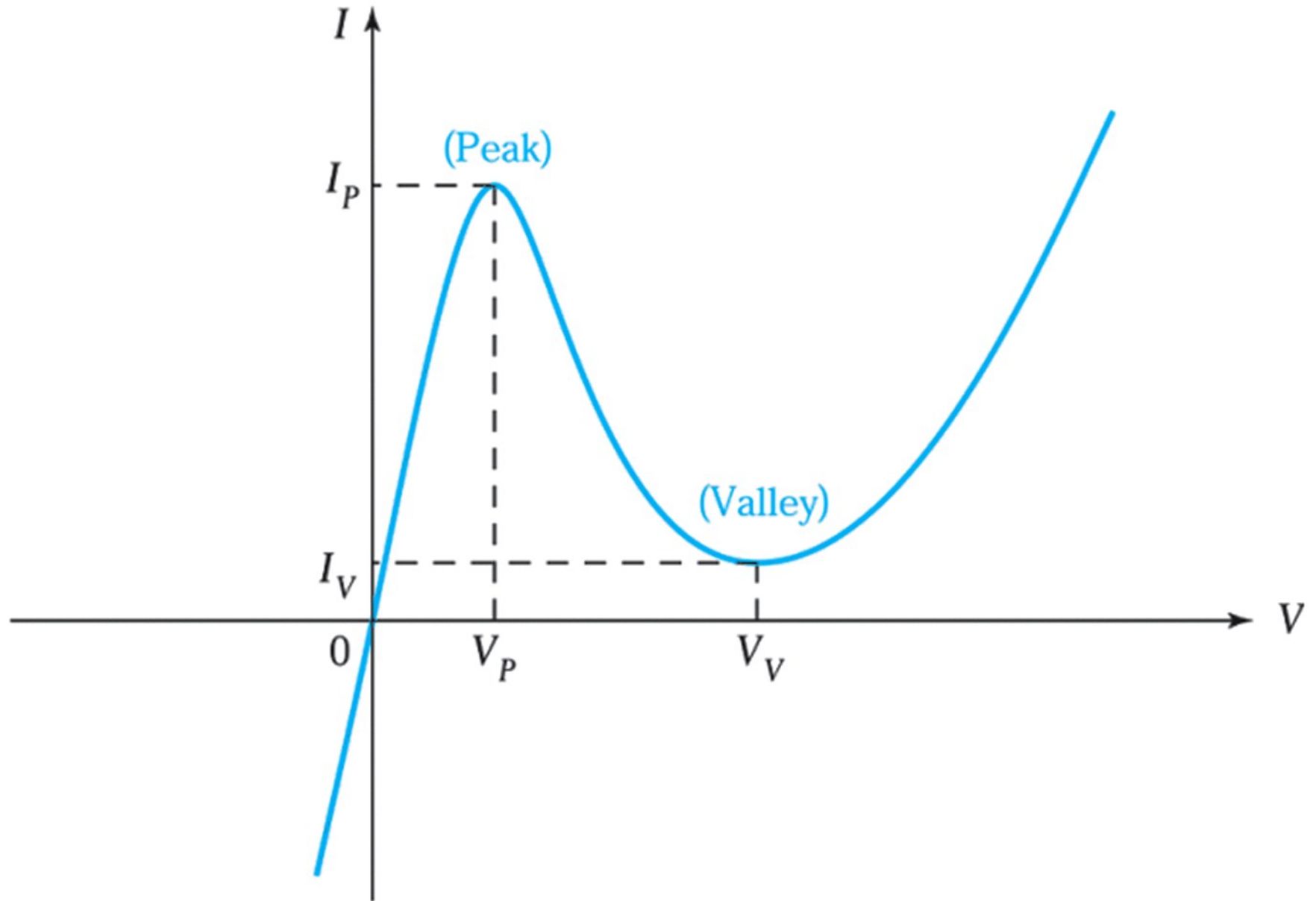
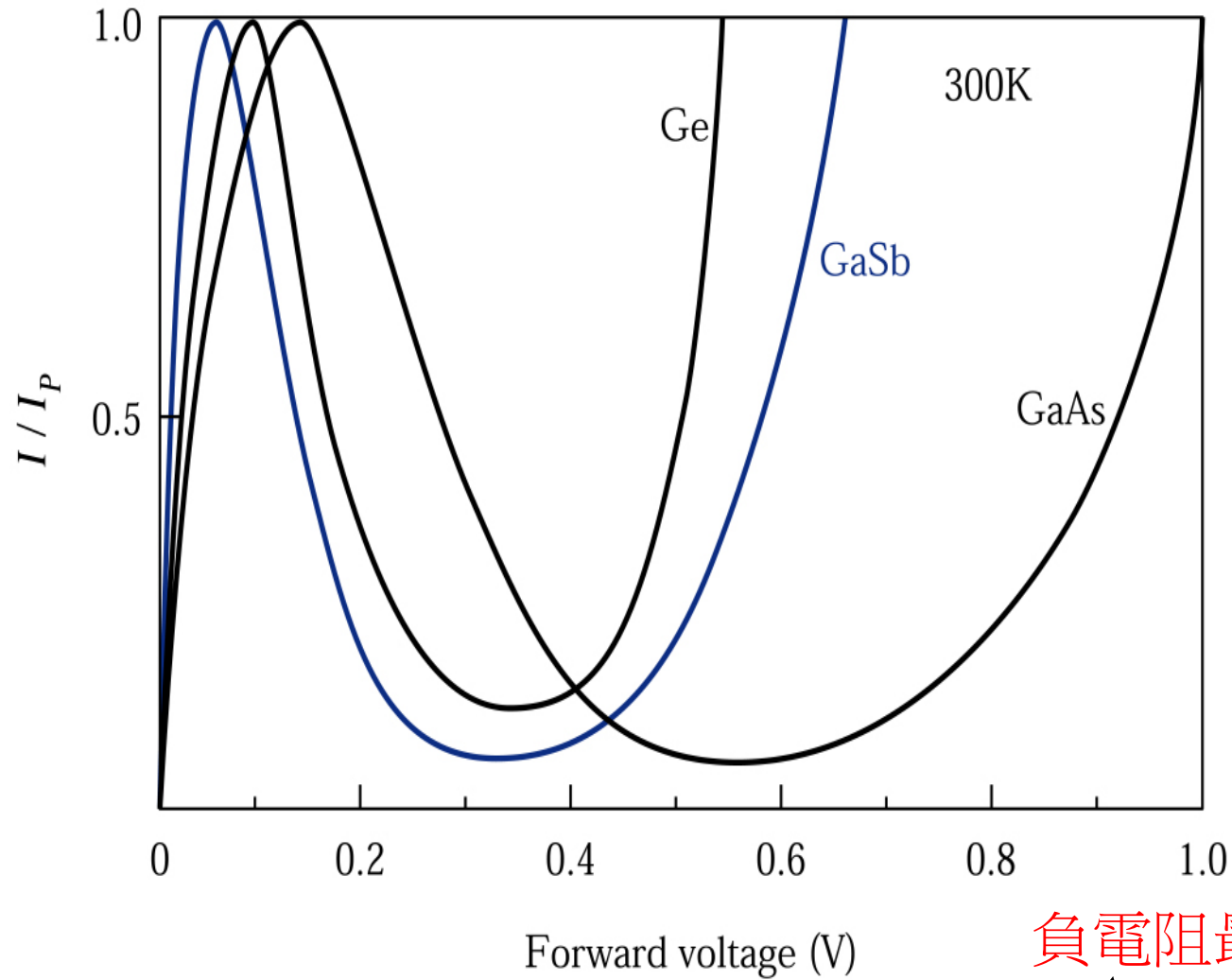


Figure 8.1 part 2  
© John Wiley & Sons, Inc. All rights reserved.



**Figure 8.2.** Typical current-voltage characteristics of Ge, GaSb, and GaAs tunnel diodes at room temperature.

# IMPATT:

## Impact Ionization Avalanche Transit-Time

>30GHz  
High noise

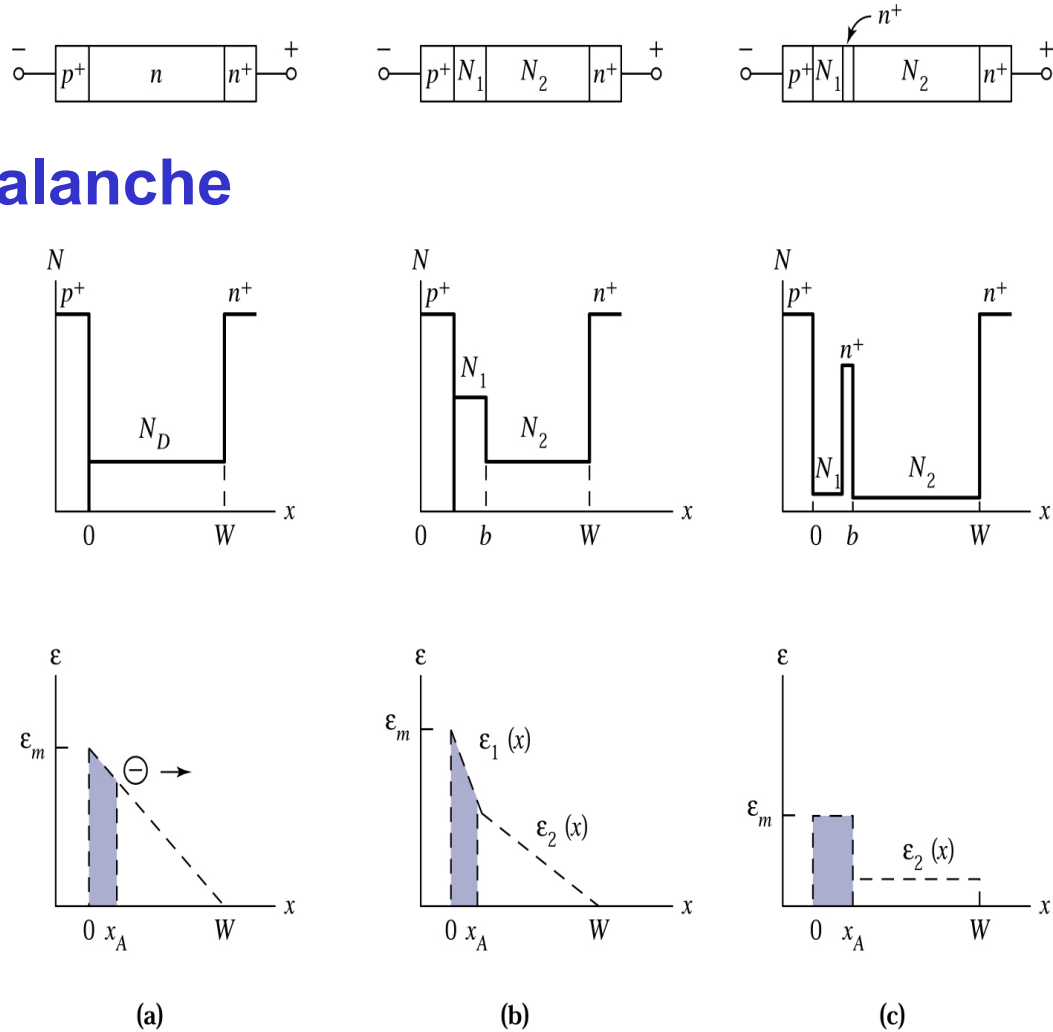
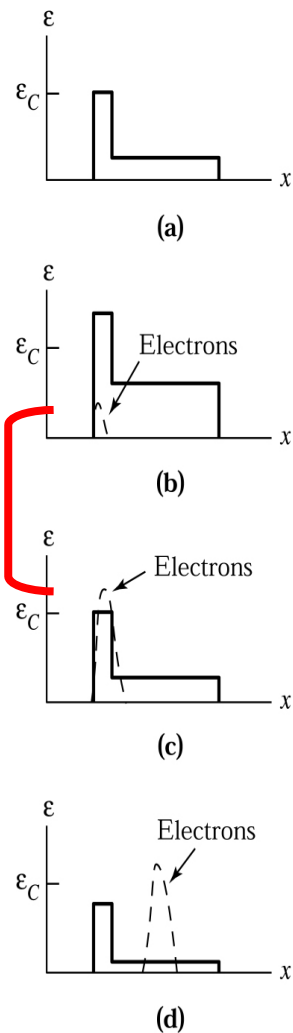


**Figure 8.3.** Doping profiles and electric-field distributions at avalanche breakdown of three single-drift IMPATT diodes: (a) one-sided abrupt  $p-n$  junction; (b) hi-lo structure; and (c) lo-hi-lo structure.

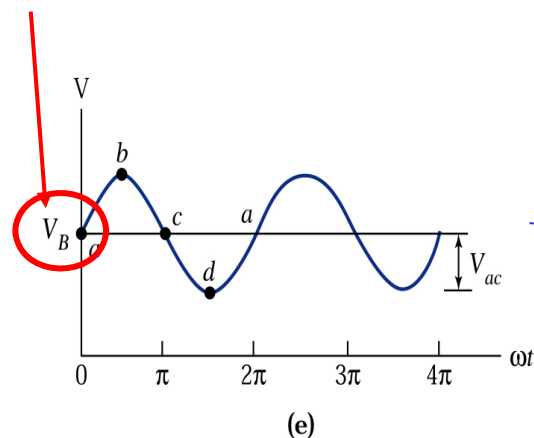


由avalanche  
變大

工作原理



逆向(皆為 reverse bias)



V↓時, I↑.  
所以負電阻.

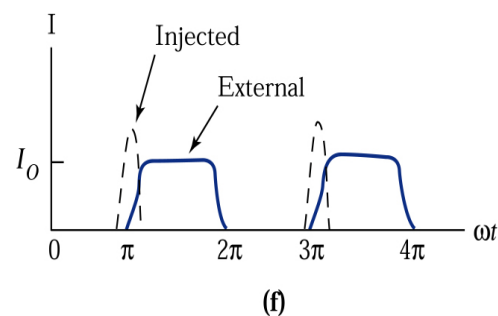
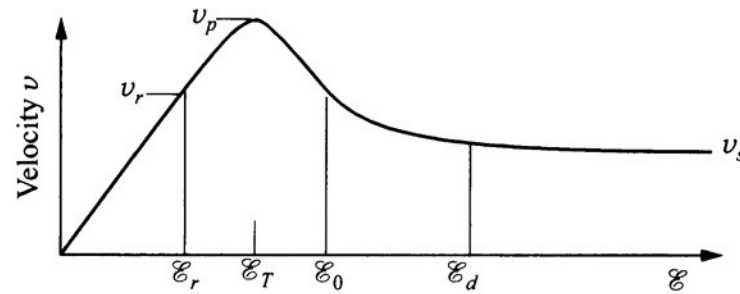


**Figure 8.4.** Field distributions and generated-carrier densities of an IMPATT diode during an ac cycle at four intervals of time (*a-d*); (*e*) the ac voltage, and (*f*) the injected and external current.<sup>7</sup>

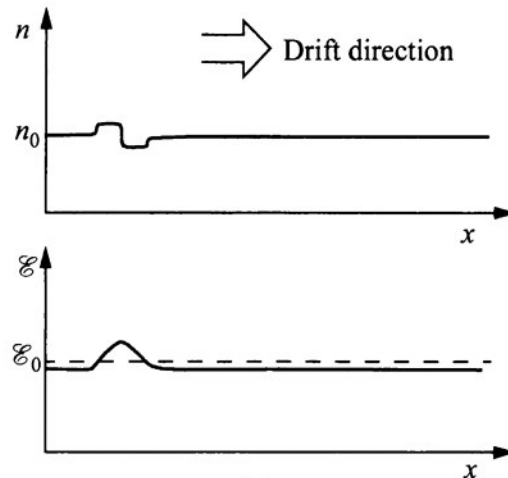
# Transfer-electron device (TED)

## Domain formation

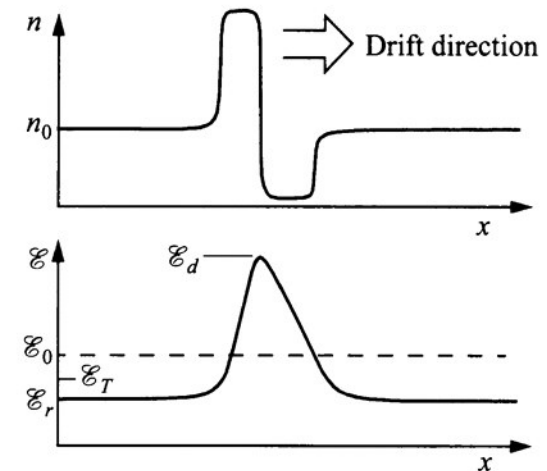
(b) Small domain grow to (c) mature domain



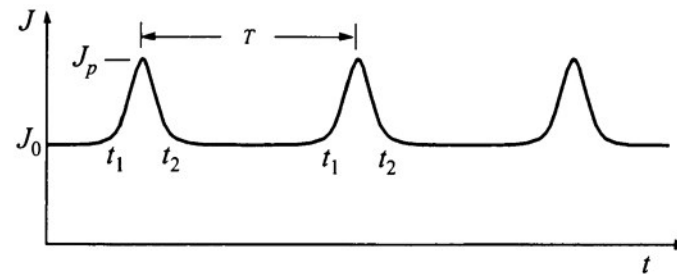
(a)



(b)

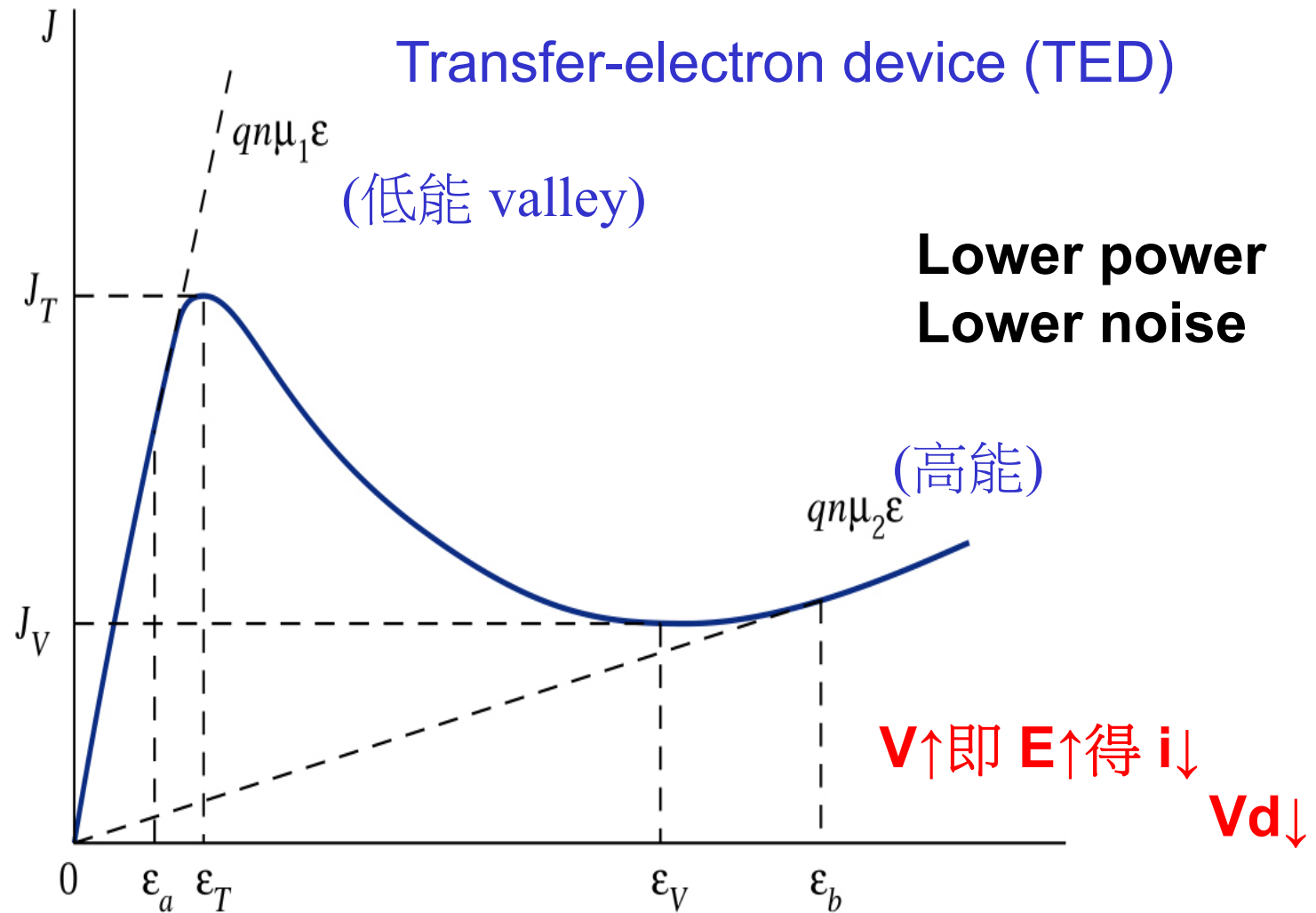


(c)



(d)

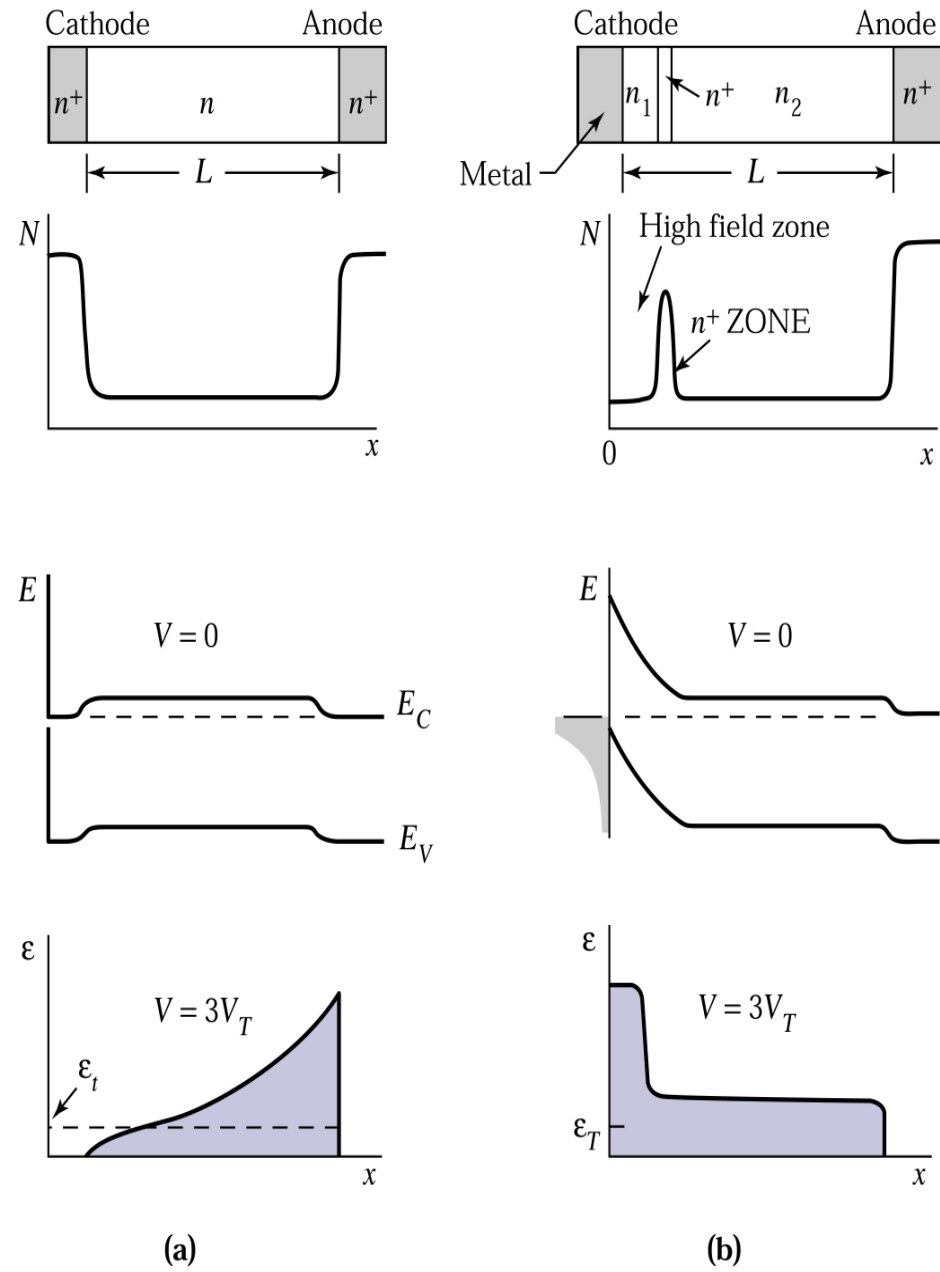
Figure 8.5  
© John Wiley & Sons, Inc. All rights reserved.



The current versus electric-field characteristic of a two-valley semiconductor.  $E_T$  is the threshold field and  $E_V$  is the valley field.

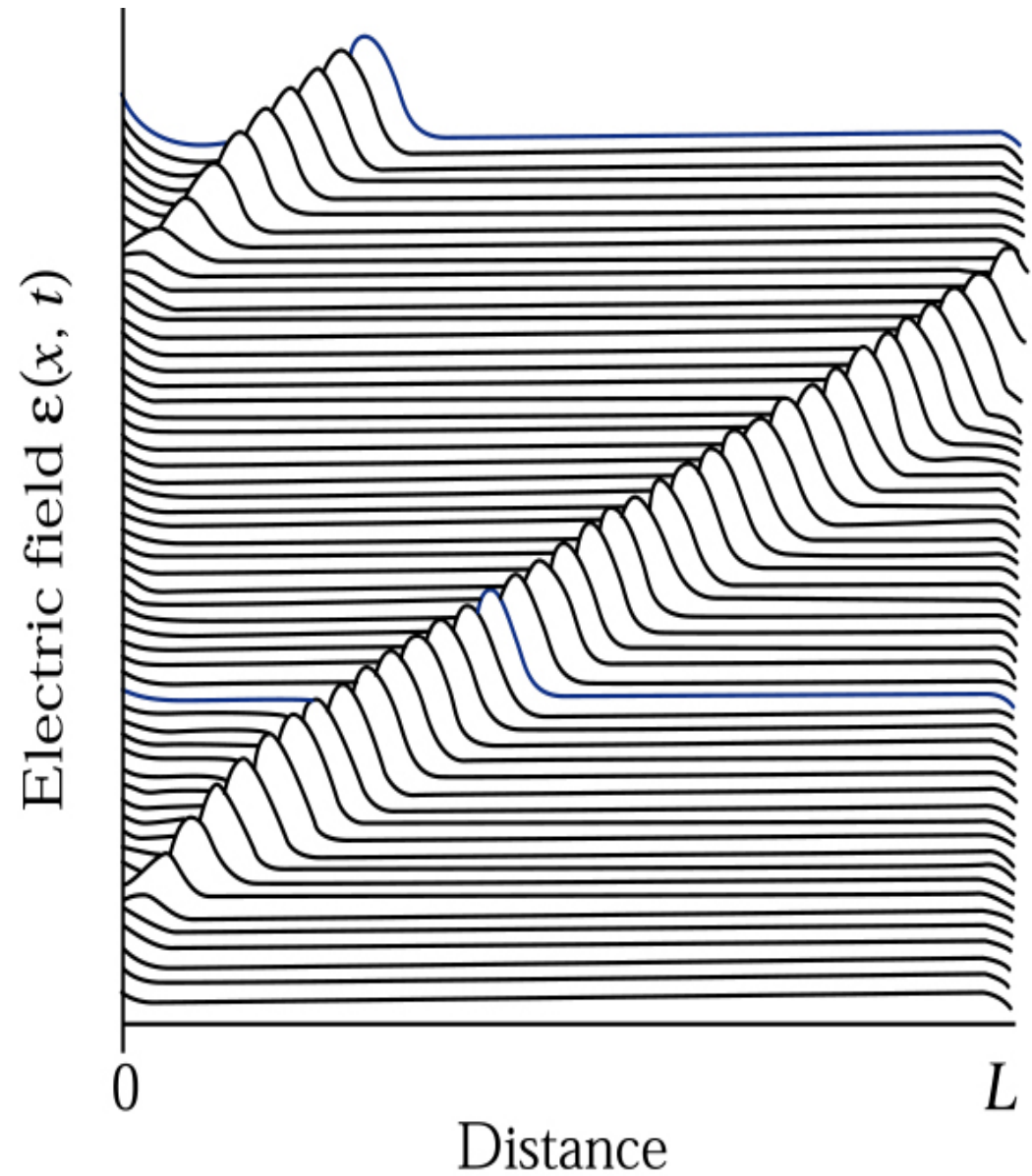
**Figure 8.6.**

Two cathode contacts for transferred-electron devices (TEDs) (a) Ohmic contact and (b) two-zone Schottky barrier contact.

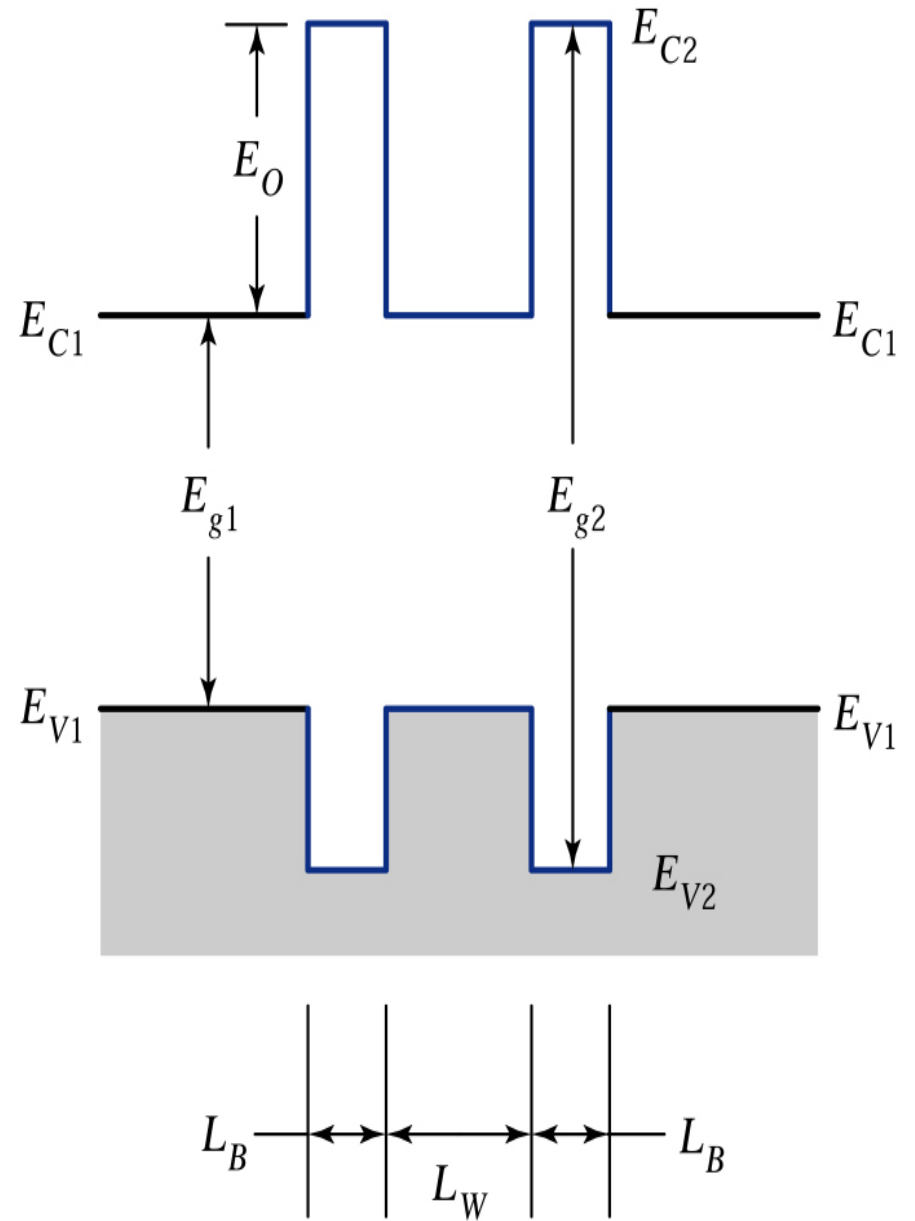


Similar to IMPATT

**Figure 8.7.**  
**Numerical simulation** of  
the time-dependant  
behavior of a cathode-  
nucleated TED for the  
transit-time domain  
mode.<sup>11</sup>



**Figure 8.8.**  
Band diagram of a  
**resonant-tunneling diode.**



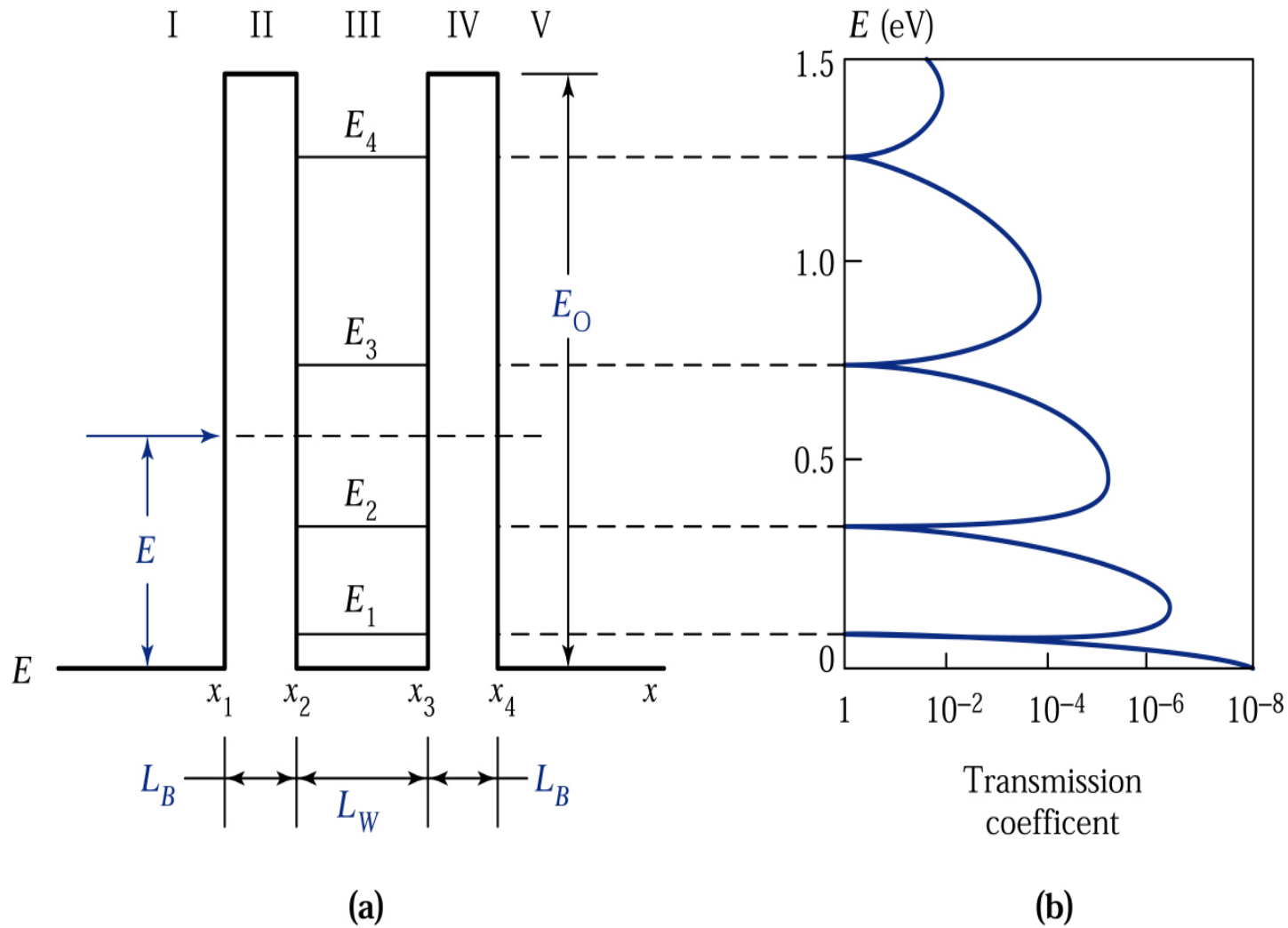
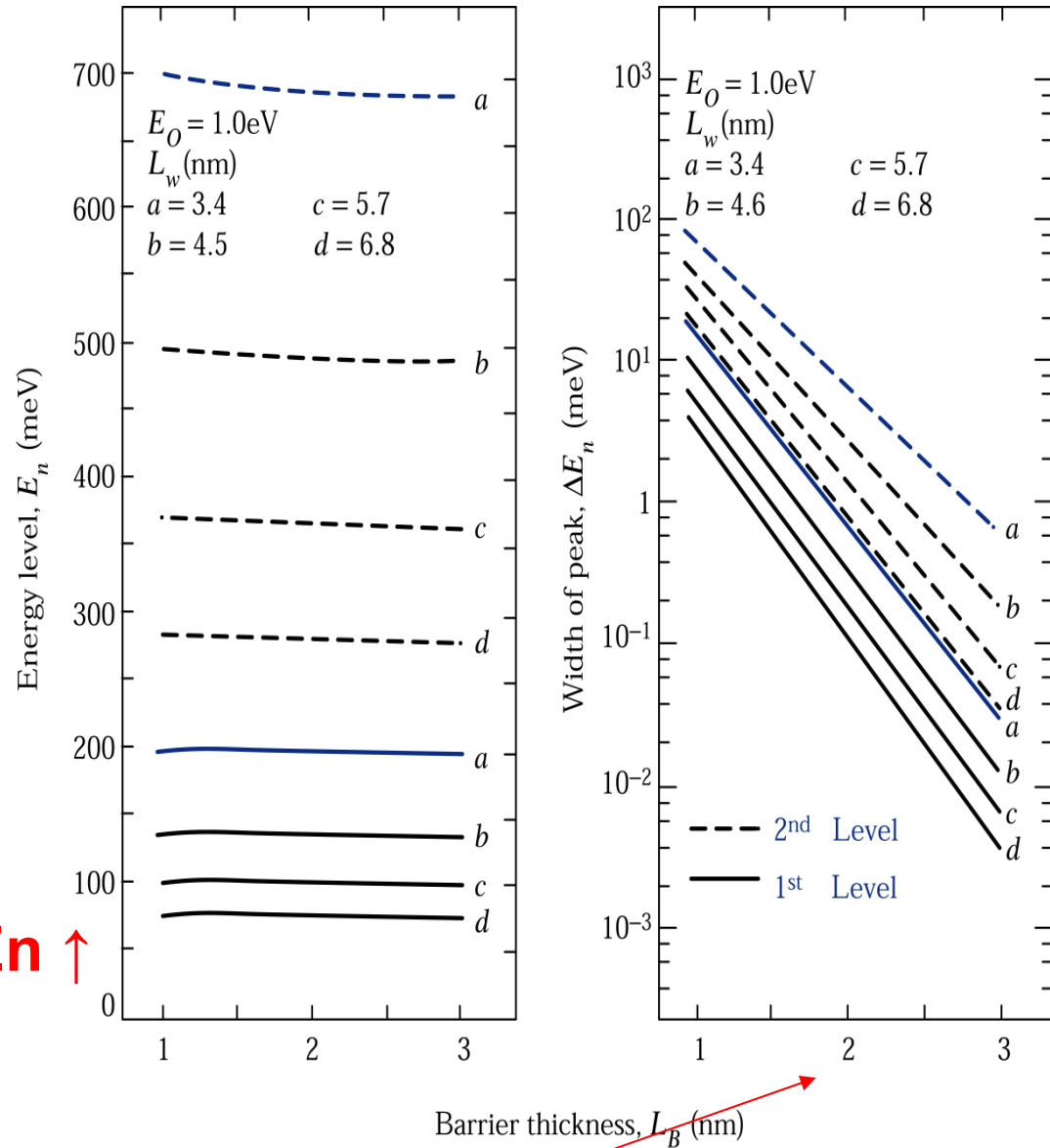


**Figure 8.9.** (a) Schematic illustration of AlAs/GaAs/AlAs double-barrier structure with a **2.5 nm barrier and a 7 nm well**. (b) Transmission coefficient versus electron energy for the structure.

**Figure 8.10.**

(a) Calculated energy of electrons at which the transmission coefficient shows the resonant peak in an AIAs/GaAs/AIAs structure as a function of barrier thickness for various well thicknesses. (b) Full width at half maximum of the transmission coefficient versus barrier thickness for the first and second resonant peak.<sup>13</sup>



**Well thickness  $L_w \downarrow \Rightarrow E_n \uparrow$**

**Barrier thickness  $L_B \uparrow \Rightarrow \Delta E_n \downarrow$**

(a)

(b)



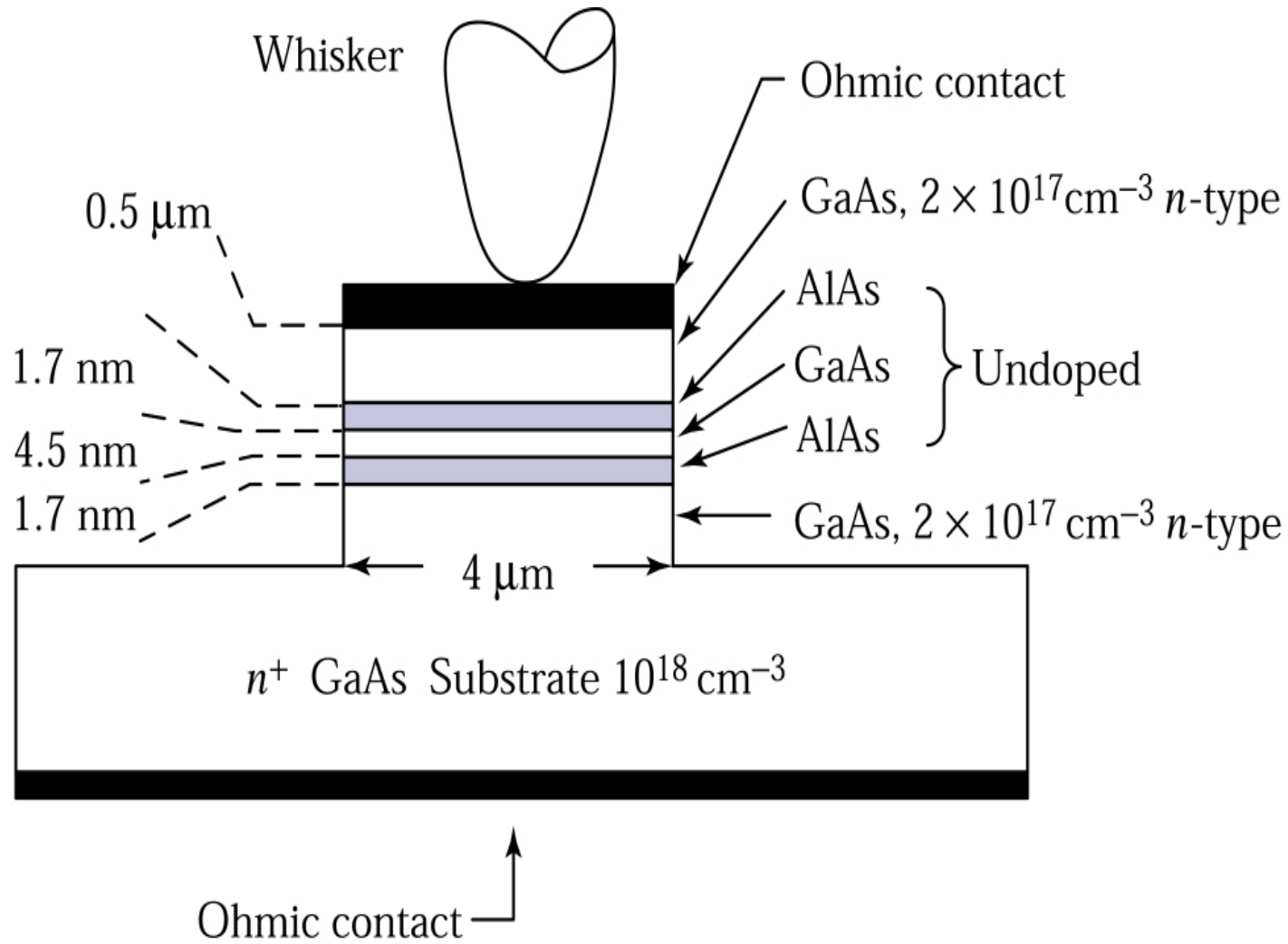


**Figure 8.11.** A mesa-type resonant tunneling diode.

**Figure 8.12.**  
Measured current-voltage characteristics<sup>13</sup>  
of the diode in Fig. 8-15.

注入電子能量 =  $E_1$

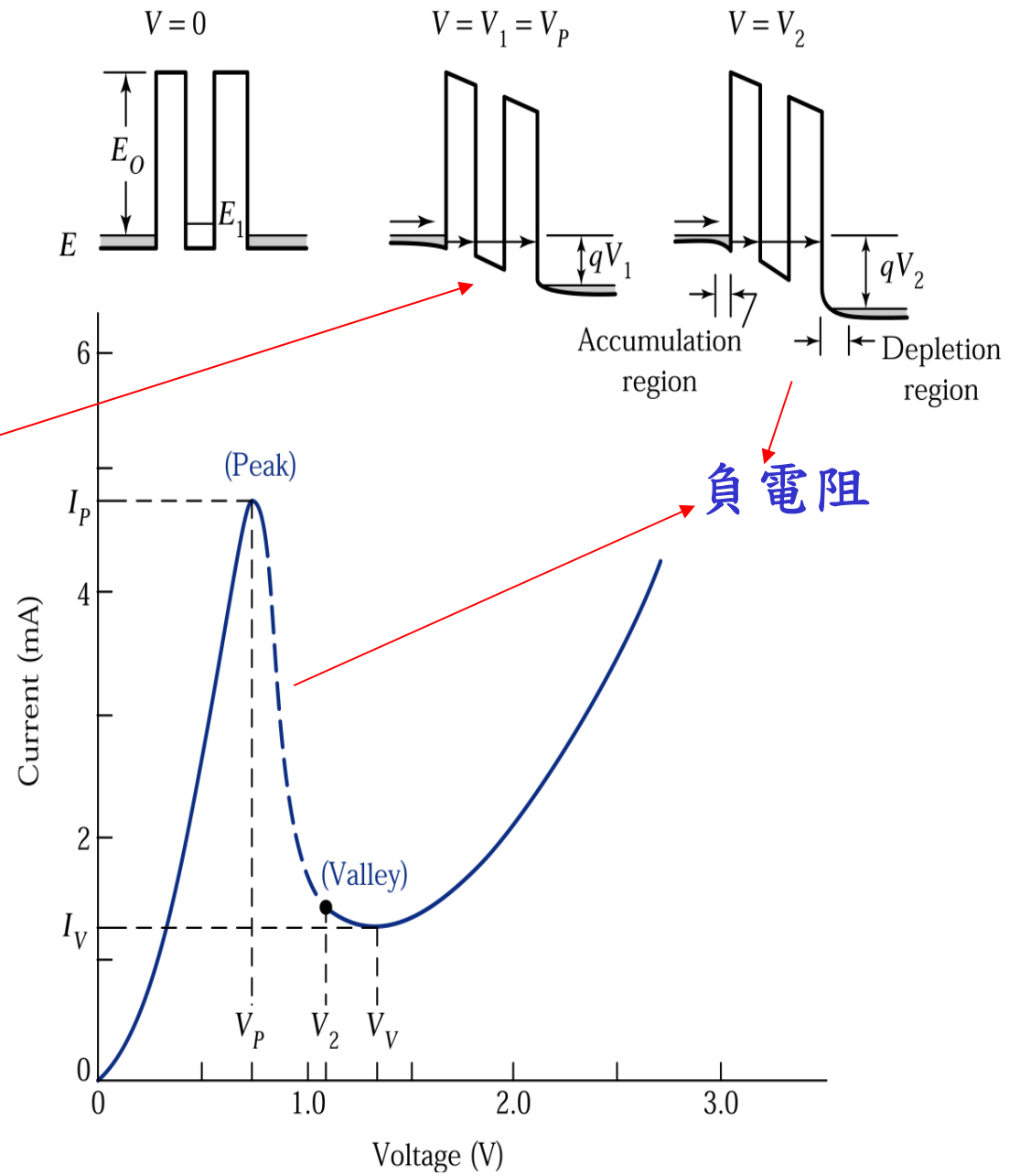
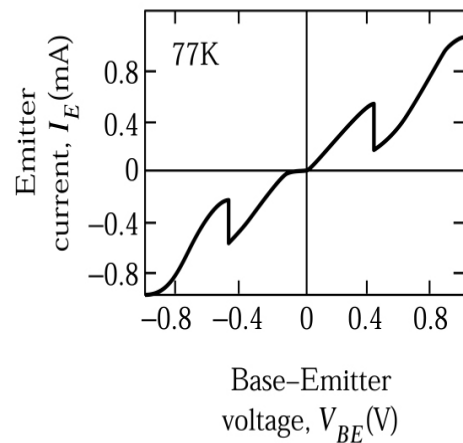
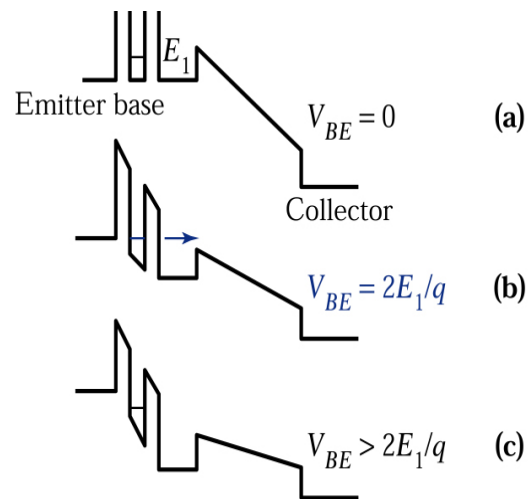
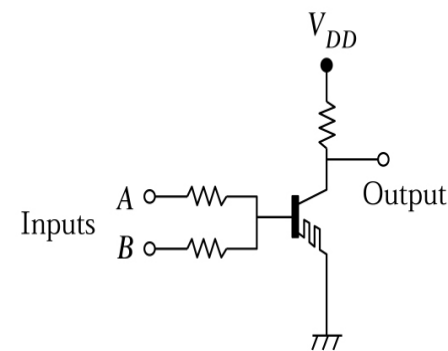


**Figure 8.13.**

Band diagrams of a unipolar resonant tunneling (RT) transistor<sup>14</sup> a (a)  $V_{BE} = 0$ , (b)  $V_{BE} = 2E_1/q$  (maximum RT current), (c)  $V_{BE} > 2E_1/q$  (RT quenched), (d) base-emitter current-voltage characteristics measured at 77 K, and (e) an exclusive NOR circuit.



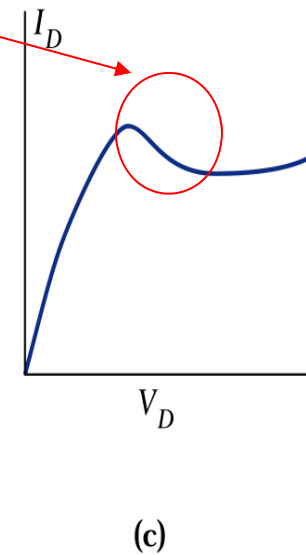
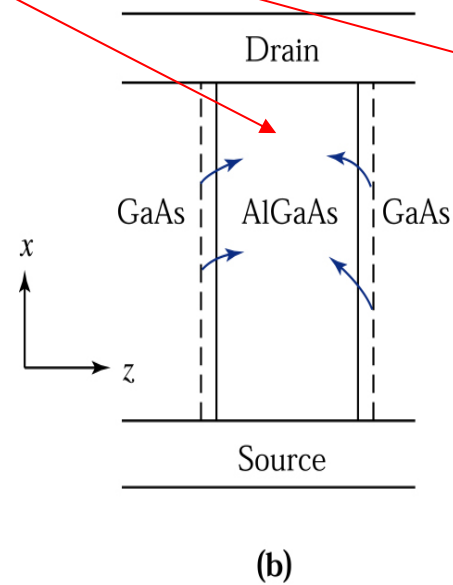
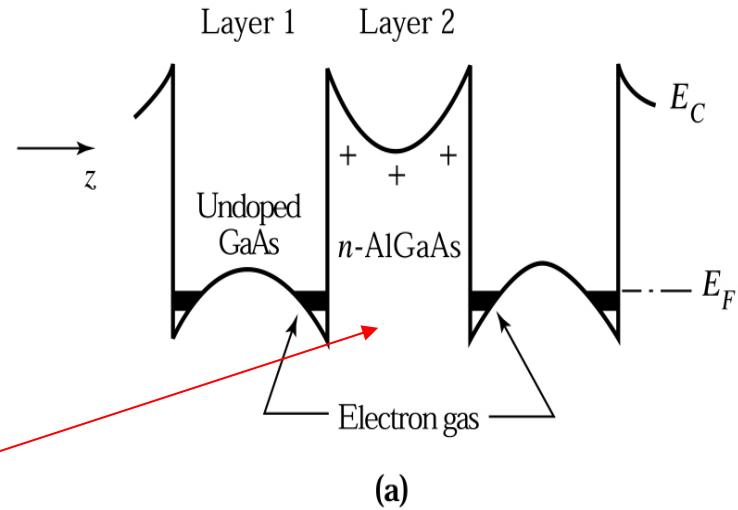
(d)



(e)

**Figure 8.14.**

(a) A heterostructure with alternate GaAs and AlGaAs layers. (b) Electrons, heated by an applied electric field, transfer into the wide-gap layers. (c) If **the mobility in layer 2 is lower**, the transfer results in a negative differential conductivity.



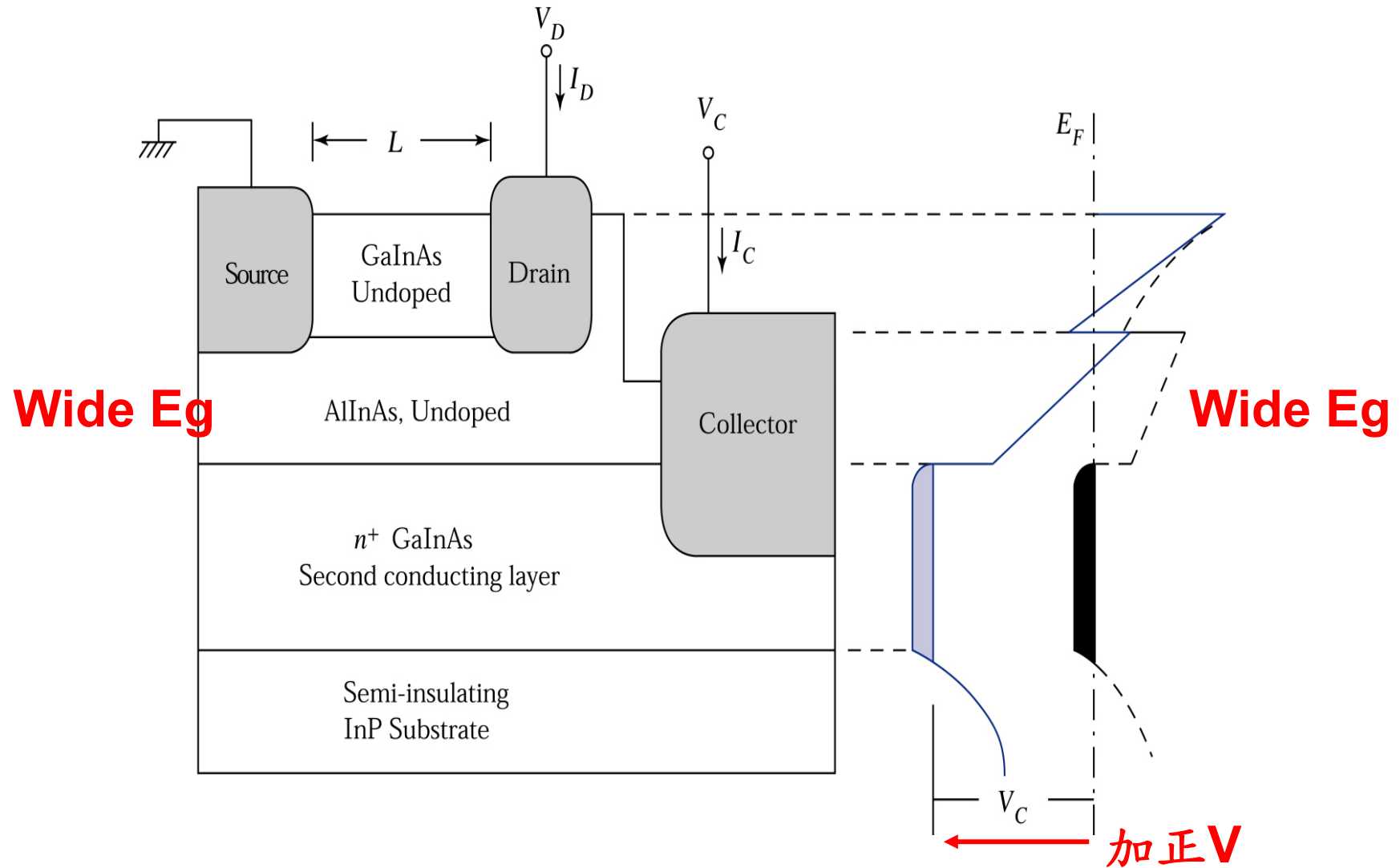
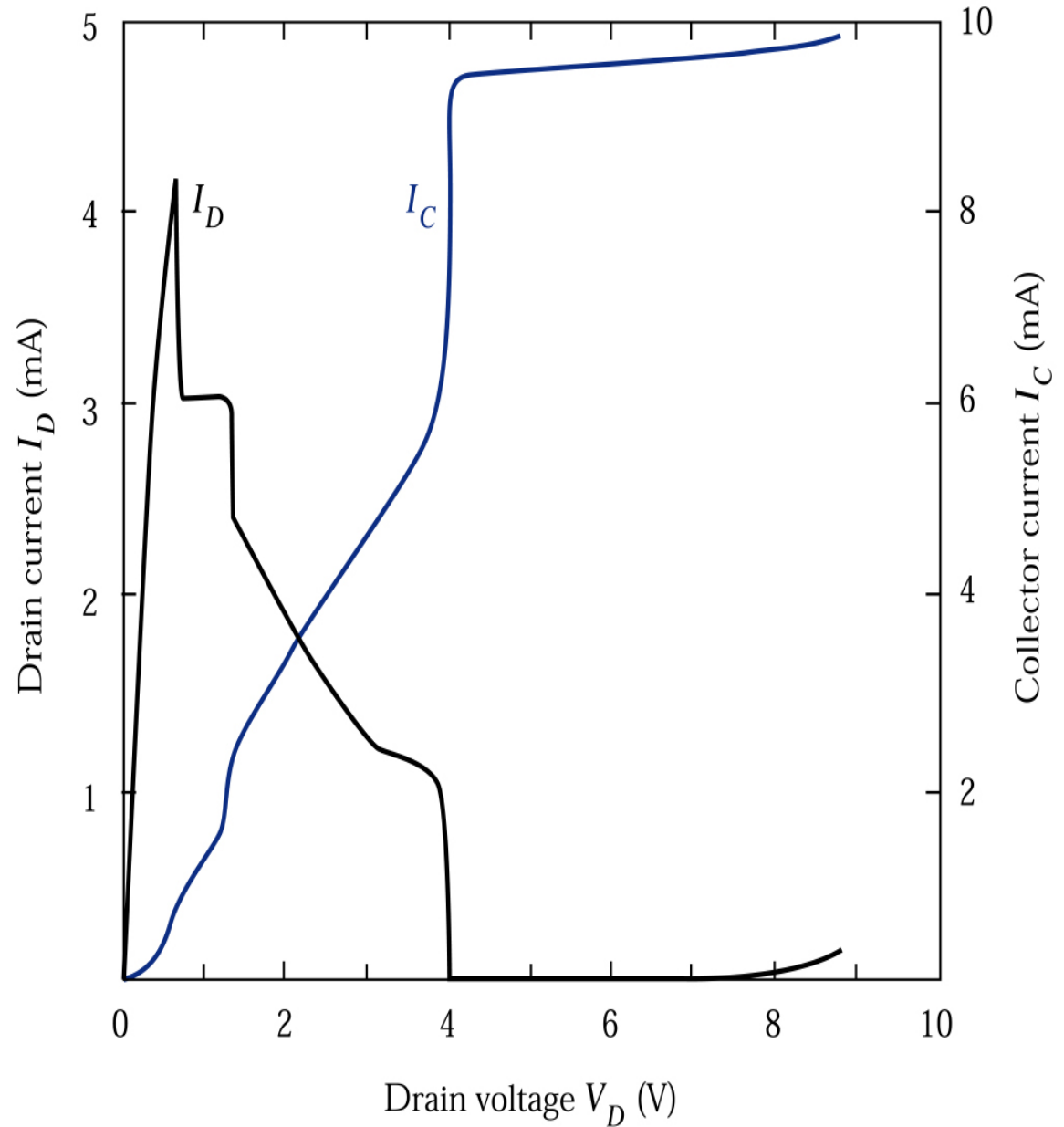


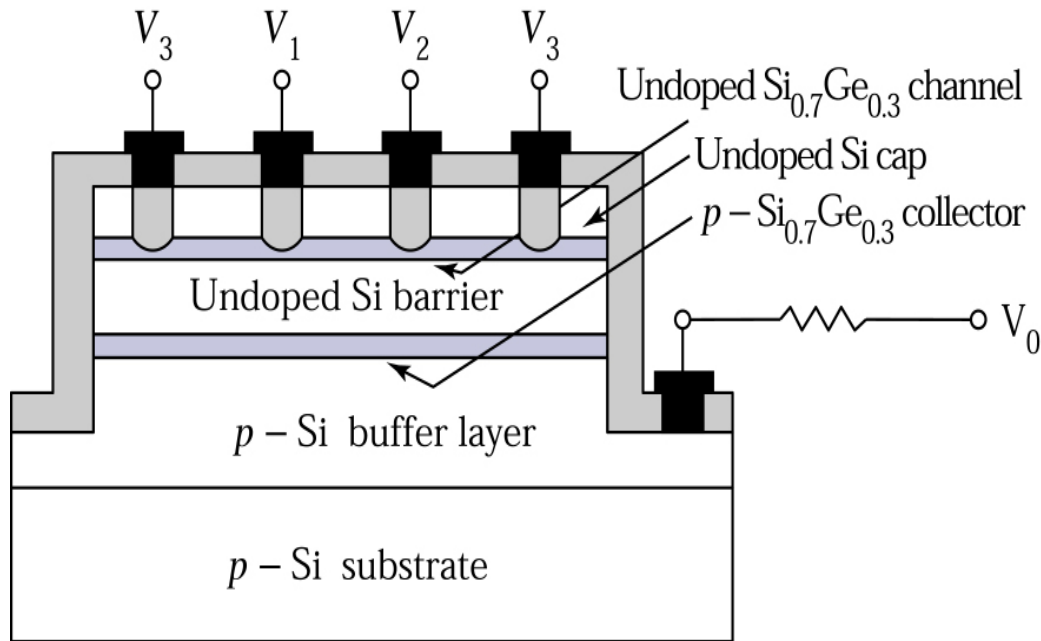
**Figure 8.15.** Cross section and band diagram of a real-space-transfer transistor in a GaInAs/AlInAs material system.

**Figure 8.16.**

Experimental real-space-transfer transistor characteristics<sup>19</sup> at  $T = 300$  K. Drain current  $I_D$  and collector current  $I_C$  versus drain voltage  $V_D$  at a fixed collector voltage  $V_C = 3.9$  V.

**$I_C \uparrow$ ,**  
 **$I_D$  流過wide  $E_g$ ,**  
 **$\mu \downarrow$ ,  $I_D \downarrow$**





(a)

$V_1$	$V_2$	$V_3$	$V_0$	Logic
0	0	0	0	O R
1	0	0	1	
0	1	0	1	
1	1	0	1	
0	0	1	1	N A N D
1	0	1	1	
0	1	1	1	
1	1	1	0	

(b)

(a) A Si/SiGe RSTT OR-NAND gate with three inputs. The channel length between different inputs is  $1 \mu\text{m}$ , and the device width is  $50 \mu\text{m}$ . (b) Truth table for OR-NAND logic operation.<sup>20</sup>